Precision Measurement of the Decay Rate of ^{7}Be in Host Materials

Y. Nir-El[1], G. Haquin[1], Z. Yungreiss[1], M. Hass[2], G. Goldring[2], S.K. Chamoli[2], B.S. Nara Singh[2], S. Lakshmi[2], U. Köster[3,4], N. Champault[3], A. Dorsival[3], G. Georgiev[3,5], V.N Fedoseyev[3], B.A. Marsh[6], D. Schumann[7], G. Heidenreich[8], S. Teichmann[8]

[1] *Radiation Safety Division, Soreq Nuclear Research Centre, Yavne, Israel*
[2] *Department of Particle Physics, Weizmann Institute of Science, Rehovot, Israel*
[3] *ISOLDE, CERN, Geneva, Switzerland*
[4] *Institut Laue Langevin, Grenoble, France*
[5] *CSNSM, CNRS/IN2P3; Univ Paris-Sud, ORSAY-Campus, France*
[6] *Physics Department, University of Manchester, Manchester, UK*
[7] *Laboratory of Radiochemistry, Paul Scherrer Institute, Villigen, Switzerland*
[8] *Target Facilities and Active Technique Section, Accelerator Division, Paul Scherrer Institute, Villigen, Switzerland*

(Dated: December 19, 2013)

A controlled and precise determination of the cross-sections of the fusion reactions ^{7}Be(p,γ)^{8}B and ^{3}He(^{4}He,γ)^{7}Be, which play an important role in determining the solar neutrino flux, necessitates the knowledge of a precise value of the electron-capture half-life of ^{7}Be. This half-life may depend on the material hosting the ^{7}Be atoms via small modifications of the electron density around the ^{7}Be nucleus. In this brief communication we report on the measurement of ^{7}Be implanted in four materials: copper, aluminum, sapphire and PVC. The four results are consistent with a null host dependence within two standard deviations and their weighted average of 53.236(39)d agrees very well with the adopted value in the literature, 53.22(6)d. The present results may exhibit a slight (0.22%) increase of the half-life at room temperature for metals compared to insulators that requires further studies.

PACS numbers: PACS 25.40.Lw, 26.20.+f, 26.65.+t

The decay rate of radioactive nuclei that undergo orbital Electron Capture (EC) depends on the properties of the atomic electron cloud around the nucleus. Hence, EC may exhibit varying decay rates if the nucleus is implanted into host materials with different properties of their corresponding electron clouds. The first suggestion of this effect in ^{7}Be, which is the lightest nucleus that decays by EC, and reports of experiments trying to investigate this phenomenon, have been presented by Segrè et al. [1, 2, 3]. This effect has been qualitatively attributed in the past to the influence of the electron affinities of neighboring host atoms [4]. The electron density of the ^{7}Be atom in a high-electron affinity material such as gold is decreased via the interaction of its 2s electrons with the host atoms, resulting in a lower decay rate (longer half-life). Recently, the life-time modification has been suggested to stem from differences of the Coulomb screening potential [5] between conductors and insulators (see below).

Several experimental and theoretical investigations were conducted during recent years to study the host material effect on the decay rate of ^{7}Be [4, 6, 7, 8, 9, 10], with a somewhat confusing scattering of experimental results. It was found that the half-life of ^{7}Be encapsulated in a fullerene C_{60} cage and ^{7}Be in Be metal is 52.68(5) and 53.12(5) days, respectively, amounting to a difference of 0.83(13)% [9]. A smaller effect of $\approx$0.2% was measured for the half-life 53.64(22) d of ^{7}Be in C_{60} and 53.60(19) d of ^{7}Be in Au [10]. A recent theoretical evaluation shows that short and long half-lives 52.927(56)d and 53.520(50)d were measured for ^{7}Be in Al_2O_3 and ^{7}Be in (average of BeO, BeF_2 and $Be(C_5H_5)_2$), respectively [4]. These results yield the magnitude of the effect to be as large as 1.1%. Another experimental investigation has shown that the half-life increases by 0.38% from ^{7}Be in graphite, 53.107(22) d, to ^{7}Be in Au, 53.311(42) [7], while a very recent investigation [11] has seen no effect to within 0.4%. The great interest in this phenomenon for ^{7}Be arises also from the need to explore the possible contribution of the half-life of ^{7}Be to the measurement of the cross section of the two fusion reactions, ^{7}Be(p,γ)^{8}B and ^{3}He(^{4}He,γ)^{7}Be, that play an important role in determining the solar neutrino flux [12, 13].

The present work has been undertaken in order to probe this phenomenon yet again in an experimental approach that takes full advantage of the experience gained in measuring implanted ^{7}Be activity in a controlled and precise manner for cross section determinations of the

solar fusion reactions mentioned above [12, 13]. As a demonstration of the quality of the γ-activity measurement, we cite the results of [12, 15] where two independent determinations of the *absolute* activity of ^{7}Be, at the Soreq laboratory and at Texas A&M University, were in excellent agreement to within 0.7%. The same setup has also been used for determining the ^{7}Be activity ensuing from the ^{3}He(^{4}He,γ)^{7}Be reaction [13]. We report the measurement of the half-life of ^{7}Be implanted in four host materials: copper, aluminum, aluminum oxide (sapphire - Al_2O_3) and PVC (polyvinyl chloride - $[C_2H_3Cl]_n$]).

The primary source of ^{7}Be for implantation was a graphite target, from the Paul Scherrer Institute (PSI), used routinely for the production of π mesons [14]. Many spallation products are accumulated in the target, including ^{7}Be. Graphite material from the PSI meson production target was placed in an ion-source canister and was brought to ISOLDE (CERN); ^{7}Be was extracted at ISOLDE by selective ionization using a resonance laser ion source. Direct implantation of ^{7}Be at 60 keV in the host material was subsequently followed. A detailed description of the extraction and implantation of ^{7}Be at ISOLDE is provided in detail in Refs. [15, 16]. This procedure facilitated a precision measurement of the cross section of the reaction ^{7}Be(p,γ)^{8}B. The implantation spot was defined by a 2 mm collimator positioned at close proximity to the target for the Cu sample and a 5 mm collimator for the other samples. This small change in the ensuing counting geometry has been well investigated for the measurement of ^{7}Be activity [13] and does not affect the results in any significant manner. The implantation process provided full control of the spot composition (^{7}Be; ^{7}Li) as well as a radial and depth profiles. For earlier implantations, at a density of ^{7}Be in Cu far exceeding that of the present experiment, the spot was found to be robust and the ^{7}Be inventory in the spot was stable [15, 17], excluding naturally radioactive decay. The copper, aluminum and PVC host material targets consisted of disks of 12 mm diameter and 1.5 mm thickness, while the sapphire target was a square of 10.2 mm x 10.2 mm. The median implantation depth of ^{7}Be into these materials has been estimated using the SRIM code [18] and found to be 12, 24, 470 and 37 μm, respectively, i.e. all implantation depths were well below the surface.

Reproducible counting geometry of the ^{7}Be samples was achieved by attaching them to plastic holders which were mounted precisely on the detector endcap. Also attached to the holders was a ^{133}Ba source ($T_{1/2} = 3841(7)$ d [19]) to correct for variations in the performance of the detection system (geometry, detection efficiency). In a separate set of measurements, an external ^{137}Cs source ($T_{1/2} = 30.03(5)$y [19]) was attached to a similar holder and thus used to estimate the reproducibility of source position by successive mountings of that holder.

Gamma-ray spectra were acquired by a p-type coaxial HPGe detector of 63.7% relative detection efficiency, 1.78 keV energy resolution (FWHM) and 81.6 peak/Compton ratio, all specified at the 1332.5 keV gamma-ray of ^{60}Co. The detector was enveloped by a 5.1 cm mercury cylinder and placed within a 10.2 cm thick lead shield. The electronic train following the detector consisted of standard units, followed by a 8192 channels multichannel analyzer.

^{7}Be decays by EC to the ground and first excited state of ^{7}Li at 477.6 keV. The branching ratio to ^{7}Li*(477.6) is 10.44(4)% and the adopted half-life is 53.22(6) d [20]. This general-use value of the half-life was intended by the evaluator, the late R. Helmer, to be valid for Be and BeO samples and adequate for various chemical forms [20].

Measurements of all ^{7}Be samples were repeated approximately every two weeks and the total decay time between the beginnings of first and last measurements of a sample was 171.1 (copper), 146.0 (PVC), 163.0 (aluminum) and 180.6 d (sapphire). Measurements were stopped when the statistical uncertainty of the 477.6 keV peak reached 0.15 to 0.10 %. At the beginning of the measurements, the activities of each sample were: 1900, 1800, 2600 and 3700 Bq, respectively and a typical counting duration was 16 hours.

Since the extracted half-life values may depend slightly on the analysis method used to compute peak areas, we describe in some detail one such procedure of data analysis that was used to extract the present results. Other analysis procedures were tried as well, without affecting the conclusions in any significant manner.

The net number of counts in the 477.6 keV peak of ^{7}Be was calculated by summation after the integral counts of the two scaled broad flat windows, to the left and right of the peak, were subtracted from the gross integral counts in the Region Of Interest (ROI) of the peak, as can be seen in Fig. 1.

The edges of the windows were determined to avoid overlap with the peaks at 437.0 keV (sum of 81.0 and 356.0 keV of ^{133}Ba) and 511.0 keV (annihilation) and the ROI was determined to include the low- and high-energy tails of the peak (see Fig. 2).

The gross number of counts in the ROI is given by: $G = G_1 + G_2 + g$ where g is the number of counts in the channel at the top of the peak.

The baseline to be subtracted is

$$B = \frac{m_1 + 0.5}{n_1} B_1 + \frac{m_2 + 0.5}{n_2} B_2 \qquad (1)$$

The net number of counts and its standard uncertainty are $N = G - B$ and $\sigma(N) = [G + \sigma^2(B)]^{0.5}$ where the variance of the baseline is given by

$$\sigma^2(B) = \left(\frac{m_1 + 0.5}{n_1}\right)^2 B_1 + \left(\frac{m_2 + 0.5}{n_2}\right)^2 B_2 \qquad (2)$$

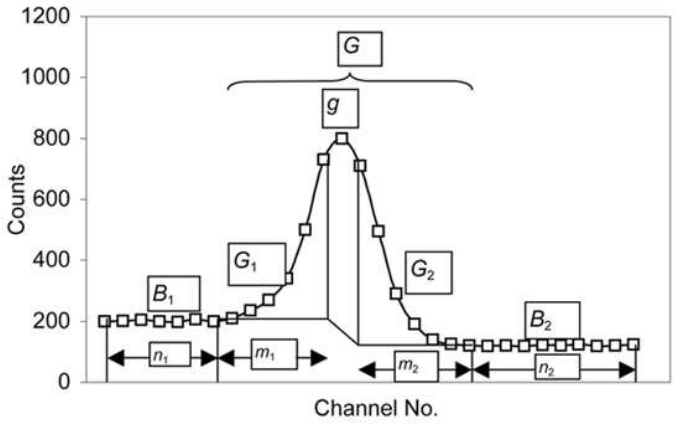

FIG. 1: Definition of 4 regions for the calculation of a net peak area by the summation method. The widths are n_1, m_1, m_2 and n_2 (in channels) and the integral numbers of counts are B_1, G_1, G_2 and B_2, respectively, depicting the case where at the top there is a single channel of g counts.

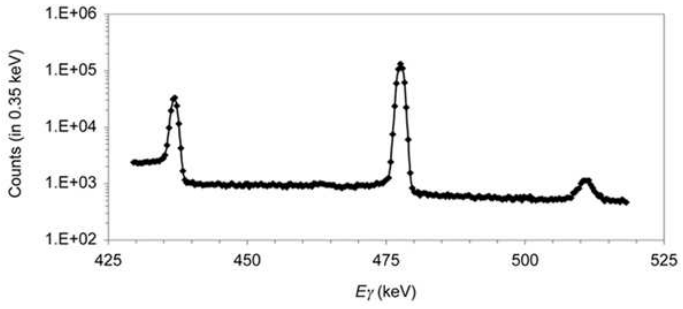

FIG. 2: An expanded view (in logarithmic scale) around the ^{7}Be peak at 477.6 keV. The quality of the γ spectrum, the two flat regions around the ^{7}Be line and the absence of any interfering γ lines can be well discerned.

If the peak is symmetrical, i.e. two channels of equal height at the top, then $g = 0$ and the 0.5 terms in Eqs. (1) and (2) must be removed.

The peak count-rate at the beginning of data acquisition is given by

$$R_0 = \frac{\lambda N}{1 - [exp(-\lambda T)]} \qquad (3)$$

where T is the acquisition Real-Time (in s) and the decay constant (in s^{-1}) of ^{7}Be is $\lambda = \frac{ln(2)}{T_{1/2}}$. $T_{1/2}$ is the half-life (in s) of ^{7}Be and its initial value in Eq. (3) can be chosen as 53.22 d. The contributions of the small errors on T and λ to the propagated uncertainty are negligible. The standard uncertainty of R_0 is then: $\sigma(R_o) = R_o \frac{\sigma(N)}{N}$. With $R_o^{(o)}$ being the count-rate at the beginning of the first measurement ($t = 0$) of a sample, the exponential decay can be expressed by the linear relationship $ln(R_o) = ln(R_o^{(o)}) - \lambda t$. A weighted linear regression of $ln(R_0)$ versus t gives the slope λ and the standard uncertainty $\sigma(\lambda)$. Hence, $T_{1/2}$ and $\sigma(T_{1/2})$ can be obtained. The calculated value of λ was substituted in Eq. (3), instead of the initial value, and the linear regression was repeated. Convergence was achieved after one iteration. The linear fitting procedure was examined by 3 criteria: (a) the correlation coefficient r, (b) the reduced chi-square χ^2/ν, and (c) the probability $P_\chi(\chi^2, \nu)$ that any random set of n data points would yield a value of chi-square as large as or larger than χ^2. The goodness of the fit is determined by how close are the extracted criteria to the optimal values of -1, +1 and 100%. The number of degrees of freedom ν is equal to n-2 for the fitting of a straight line (the single coefficient is the slope and the constant term is the intercept).

The decay of the peak count-rate of the Al_2O_3 sample is shown as an example in Fig. 3. Uncertainties of count-rates were of the order 0.10 to 0.16% and express the high precision of the measurements. Fig. 3 shows also that the calculated straight line fits well the measured results. The goodness of the linear fit of the Al_2O_3 sample is

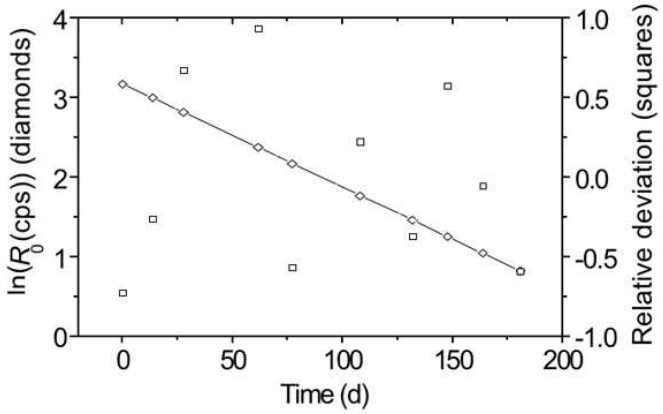

FIG. 3: Left axis - (diamonds): The decay curve of the 477.6 keV line of ^{7}Be imbedded in the Al_2O_3 sample. The straight line was fitted by a weighted linear regression. Right axis - (squares): The deviation between the measured and the fitted count rates, divided by the corresponding uncertainty, for the 10 measurements of the Al_2O_3 sample (see text).

displayed in Fig. 3, which shows the difference between measured and calculated (fitted) count-rates, in units of the associated uncertainty of the measured value.

The geometrical uncertainty, found by the ^{137}Cs source to be 0.035%, was applied to each data point in quadrature addition to the statistical uncertainty $\sigma(R_o)$. The analytical uncertainty 0.062% was determined by running three different methods to analyze a peak area. This uncertainty was added in quadrature to the provisional uncertainty as calculated by the linear regression.

The weighted average of the measured half-lives of the four host materials, presented in Table I and in Fig. 4,

TABLE I: The details of the half-life determinations and the linear regression fits for the four samples. r is the correlation coefficient defined in the text.

Host Material	n	$T_{\frac{1}{2}}(d)$	$(r+1)10^6$	χ^2_ν	$P_\chi(\chi^2,\upsilon)(\%)$
Cu	10	53.353(50)	1.9	0.94	48.56
Al	10	53.257(44)	0.9	0.73	66.53
Al_2O_3	10	53.180(43)	0.4	0.39	92.73
PVC	10	53.181(45)	1.7	1.26	25.88

is 53.236(39) d, which agrees well with the adopted value 53.22(6) d [20], with no account being taken of the host material.

Even though the statistical test of the present data supports a null effect within $\pm$ 1σ, the results of Fig. 4 may indicate a slight positive trend of the half-life versus the electron affinity, where a host material with high-electron affinity such as copper (conductor), exhibits a longer half-life, compared to a lower electron affinity material such as aluminum oxide (insulator).

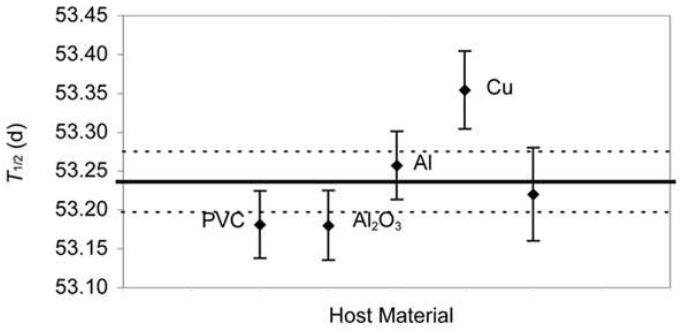

FIG. 4: The half life of ^{7}Be in 4 host materials. The solid line represents the weighted average and the broken lines correspond to a $\pm 1\sigma$ interval. Also shown is the adopted value in the literature [20]

A different possible interpretation of the life-time results follows a recent observation by Wang et al. [21] of an approximately 1% increase in the lifetime of ^{7}Be in metallic vs. insulator environments at low temperature. This change is consistent with the Debye screening model [5] that has been successfully used to explain the screening potential for nuclear reactions at very low beam energies. The average life times for the two insulators (PVC and Al_2O_3) and the two metals (Cu and Al) are 53.180(31) d and 53.299(33) d, respectively, a difference of 0.22%. Indeed, the trend of the present data is in basic agreement with the temperature dependence of the screening model, as well as with the results of [11]. A further investigation of such a small trend and its detailed temperature dependence is clearly called for.

We thank the PSI technicians Pedro Baumann and Alfons Hagel for the target handling and the ISOLDE staff for their help. The work has been supported in part by the Israel Science Foundation and the EU-RTD project TARGISOL (contract HPRI-CT-2001-50033). We acknowledge the support of the ISOLDE Collaboration.

[1] E. Segrè, Phys. Rev. **71**, 274 (1947).
[2] E. Segrè and C. E. Wiegand, Phys. Rev. **75**, 39 (1949).
[3] R.F. Leininger, E. Segrè and C. Wiegand, Phys. Rev. **76**, 897 (1949).
[4] P. Das and A. Ray, Phys. Rev. C**71**, 025801 (2005).
[5] K.U. Kettner, H.W. Beckker, F. Strieder and C. Rolfs, J. Phys. G **32**, 489 (2006); and references therein.
[6] A. Ray, P. Das, S. K. Saha, S. K. Das, B. Sethi, A. Mookerjee, C. Basu Chaudhuri, G. Pari, Phys. Lett. B**455**, 69 (1999).
[7] E.B. Norman, G.A. Rech, E. Browne, R.-M. Larimer, M.R. Dragowsky, Y.D. Chan, M.C.P. Isaac, R.J. McDonald, A.R. Smith, Phys. Lett.B**519**, 15 (2001).
[8] A. Ray, P. Das, S.K. Saha, S. K. Das, Phys. Lett. B**531**, 187 (2002).
[9] T. Ohtsuki, H. Yuki, M. Muto, J. Kasagi, K. Ohno, Phys. Rev. Lett. **93**, 112501 (2004).
[10] A. Ray, P.Das, S.K. Saha, S.K. Das, J.J. Das, N. Madhavan, S. Nath, P. Sugathan, P.V.M. Rao, A. Jhingan, Phys. Rev. C**73**, 034323 (2006).
[11] B.N. Limata et al., Eur. Phys. J. A**27**, s01, 193-196 (2006).
[12] L. T.Baby et al., Phys. Rev. Lett. **90**, 022501 (2003).
[13] B.S. Nara Singh, M. Hass, Y. Nur-El, G. Haquin, Phys. Rev. Lett. **93**, 262503 (2004).
[14] G. Heidenreich, Proc. AIP **642**, 122 (2002).
[15] L.T. Baby et al., Phys. Rev. C**67**, 065805 (2003).
[16] U. Köster, M. Argentini, R. Catherall, V. N. Fedoseyev, H. W. Göggeler, O. C. Jonsson, R. Weinreich and ISOLDE Collaboration, Nuc. Inst. Meth. B**204**, 343 (2003).
[17] M. Hass et al., Phys. Lett. B**462**, 237 (1999).
[18] SRIM package from www.srim.org
[19] J.K. Tuli, Nuclear Wallet Cards, 7th ed., (2005), www.nndc.bnl.gov
[20] D.R. Tilley, C.M. Cheves, J.L. Godwin, G.M. Hale, H.M. Hofmann, J.H. Kelley, C.G. Sheu, H.R. Weller, Nucl. Phys. A**708**, 3(2002).
[21] B. Wang et al., Eur. Phys. J. A**28**, 375-377; and references therein (2006).